

Received March 15, 2021, accepted March 28, 2021, date of publication April 6, 2021, date of current version April 19, 2021.

Digital Object Identifier 10.1109/ACCESS.2021.3071340

Performance Enhancement of PV System Configurations Under Partial Shading Conditions Using MS Method

SNIGDHA SHARMA¹, LOKESH VARSHNEY¹, RAJVIKRAM MADURAI ELAVARASAN²,
AKANKSHA SINGH S. VARDHAN³, AANCHAL SINGH S. VARDHAN³,
R. K. SAKET⁴, (Senior Member, IEEE),
UMASHANKAR SUBRAMANIAM⁵, (Senior Member, IEEE),
AND EKLAS HOSSAIN⁶, (Senior Member, IEEE)

¹School of Electrical, Electronics and Communication, Galgotias University, Noida 201309, India

²Clean and Resilient Energy Systems (CARES) Laboratory, Texas A&M University, TX 77553, USA

³Department of Electrical Engineering, Shri G. S. Institute of Technology and Science, Indore 452003, India

⁴Electrical Engineering Department, Indian Institute of Technology (BHU), Varanasi 221005, India

⁵Renewable Energy Laboratory, Department of Communications and Networks, College of Engineering, Prince Sultan University, Riyadh 11586, Saudi Arabia

⁶Department of Electrical Engineering and Renewable Energy, Oregon Institute of Technology, Klamath Falls, OR 97601, USA

Corresponding authors: Rajvikram Madurai Elavarasan (rajvikram787@gmail.com) and Umashankar Subramaniam (usubramaniam@psu.edu.sa)

This work was supported by Prince Sultan University, Riyadh, Saudi Arabia.

ABSTRACT The study of this work is to highlight the key metrics of various topologies in terms of output power, Fill Factor (FF), Mismatch Losses (ML) and efficiency. The idea behind this work is to analyze and obtain the performance of different topologies under various shading patterns. The major problem which comes across the path of Photovoltaic (PV) system performance is partial shading. The solution to this problem is to reconfigure the panels to achieve better results under shading conditions. For this, different configurations such as Series Parallel (SP), Total Cross Tied (TCT), Physical Relocation of Module with Fixed Electrical Connections (PRM-FEC), SuDoKu and Magic Square (MS) has been discussed, analyzed and compared using MATLAB/SIMULINK. Simulation approach is used to describe the working and evaluation of all configurations. By the results obtained, it is clearly visible that MS method have achieved largest output power of 2877 W, highest efficiency of 10.24 %, FF is 0.481 and lowest ML of 772 W among all the configurations under Long Narrow (LnN) pattern.

INDEX TERMS Efficiency, Fill Factor, Magic Square, photovoltaic array, SuDoKu.

I. NOMENCLATURE

D	Ideality factor of diode(1.3)
E_{g0}	Band gap energy of semiconductor(eV)
I	Current(A)
I_m	Module current(A)
I_p	Photocurrent (A)
I_R	Row current(A)
I_r	Reverse saturation current(A)
IRD	Solar irradiation(W/m ²)
I_s	Short circuit current (A)
$ISTC$	Solar irradiation at STC (W/m ²)
K_b	Boltzmann's constant(J/K)

K_s	Short circuit current of a cell at standard test condition (STC)
N	Number of series cells
P	Power (W)
Q	Electron charge(C)
R_{se}	Series resistance in ohms
R_{sh}	Shunt resistance in ohms
T_n	Nominal temperature(K)
T_o	Operating temperature(K)
V	Voltage(V)
V_{oc}	Open circuit voltage(V)

II. INTRODUCTION

The associate editor coordinating the review of this manuscript and approving it for publication was Zhilei Yao^{id}.

The world is moving towards the rapid development of sustainable energy technology and solar energy possesses a vital

role in this field. Solar Photovoltaic (PV) system behaves as an environment friendly source in contrast to fossil fuels reserves. Solar energy is widely available, but extraction of this energy is limited by the efficiency factor. The performance of PV system has adverse effects due to factors such as changes in solar radiation, effects of shading and rise in temperature of solar cell. Due to these factors, the basic characteristics of solar PV system vary which leads to the variation of maximum power point (MPP) and consequently, the overall efficiency reduces.

Qing *et al.* [1] provide a model which depends upon sub module to improve the characteristics of Series Parallel (SP) configuration under different shading patterns, changing irradiance and temperature variation. A sample of submodules in addition with bypass diode are taken in the paper to evaluate Mismatch Losses (ML) in Series Parallel configuration PV array. The authors of [2] focuses mainly on series, parallel and SP PV system characteristics under various shading patterns. The parallel configuration gives maximum power output which is experimentally verified in the paper. The paper [3], [4] purpose is to analyze Series Parallel and Total Cross Tied (TCT) configuration under shading conditions. The author has considered PV system grid along with incremental conductance technique to track maximum power point quickly. MATLAB/Simulink verifies better performance of TCT with respect to SP configuration. The paper [5] analyzed SP PV array in addition with bypass diode integration for enhancing the performance. The authors evaluate performance under various conditions such as without bypass diode, single string- single bypass diode, single string- double bypass diode, series group- bypass diode, staggered group-bypass diode and multi level-octal bypass diode. According to results multi level-octal bypass diode based SP topology is ahead of remaining methods.

Michal Orkisz [6] presents poison factor which provides total panel loss if a panel gets short circuited. This concept is used on SP array to estimate the total power loss. The authors of [7] provides PV generator performance with series, parallel configuration under different irradiation and temperature. Anssi and Valkealahti [8] investigates the performance of long string, parallel string and multi string PV generator under different shading conditions. The author verified that individual short string is superior than other configurations. The paper [9] introduced a switch set based on particle swarm optimization method for series, parallel and SP configuration. The switch set is evaluated experimentally under different anomalous condition. According to the test results, less number of switches can be used with any configuration and also overcome abnormal conditions. Yuki Mochizuki *et al.* presented power generated by two identical stages with 1/3 phyllotaxis is 1.5 times of flat surface PV panel power. The Fibonacci number PV module incorporates many features such as number of stages can be increased, reflected light from one cell can be used by other cells, lesser area in shadow and impact of one cell shadow on the other. Authors introduced the new pattern of Fibonacci method based on

honeycomb (HC) structure in order to attain characteristics of power generation. According to this paper, Fibonacci based solar PV modules are located at distance of 30cm from centre solar PV module [10], [11].

The paper implemented a reconfiguration method to analyze the PV system performance under various fault condition. The method is compared with three topologies which includes Series Parallel, Total Cross Tied and bridge link (BL). It is concluded that reconfiguration method performs well with respect to other configurations under all faulty situations. The authors presents a comparison of different topologies in terms of higher power output, global and local peaks, Fill Factor (FF) and Mismatch Losses [12], [13]. A new method- Futoshiki topology is introduced, whose execution is following up concerning with TCT. The author shows enhancement of power and reduction of Mismatch Losses by means of proposed method [17] while the proposed work in this work not only analyzed four different configurations on basis of output power and Mismatch Losses but also taken Fill Factor and efficiency under consideration. Pendem *et al.* [19] introduced TCT configuration for string integrated converters along with perturb and observe technique to achieve maximum output power while the author of this work focusses only on configurations and shading patterns. The author has not involved maximum power point tracking controller along with any configuration. The objective of paper [20] is to analyze distributed maximum power point tracking from interleaved converter to extract maximum power. The proposed concept has been tested via experiment as well as simulation.

The authors of paper [21] provides a method for selecting parameters of PV system via MATLAB/SIMULINK. The paper used two modified algorithms of particle swarm optimization for getting maximum global power point. The result identified modified particle swarm optimization fulfil the requirements of PV system while this work is analyzed based on configurations to achieve maximum output power and not analyzed on maximum power point tracking controllers. Khan *et al.* [22] indulge maximum power point techniques in addition to PV system for minimizing circuit Mismatch Losses. The proposed architecture uses integrated converter to improve the system response. Both hardware and software models are examined to verify the results. The paper [23]–[25] presented flower pollination algorithm to track peaks under shading transitions. The method is also quantified with other maximum power point tracking techniques. Experimental study has been done by authors to verify results while this work presents relocation of panels to optimize configurations for obtaining higher performance and does not taken into account maximum power point tracking controller along with PV system. The authors of paper [27] introduced a new reconfiguration model with particle swarm optimization to enhance total output power under various shading conditions.

The paper [33], [34] analyze efficiency of PV system model under shading transitions and to track global maximum power point peak. The system is also analyzed on parameters

such as power and temperature. The author of [35] gives bifacial one dimensional tracking system to separate Mismatch Losses and shading losses via simulation only as experimentally its very difficult to achieve. The paper [36], [37] investigates bifacial power enhancement. The energy yield of bifacial system is also analyzed and simulated data is compared with experimental data in order to obtain final results. The experimental work in [38] on proposed PV model has been done to determine its quantities and energy production. Sangrody *et al.* [39] presents accuracy in forecasting via similarity based forecasting models. The paper [40] proposed techniques to detect the value of series resistance. For obtaining the value, five different techniques are considered along with other parameters such as dark current etc.

The PV modules are joined in different configurations for enhancing the output power. Under shading conditions, series topology starts acting as load instead of the source. The major problem of using PV system is less efficiency which is the effect of ML due to different shading patterns. So various connections came into existence in order to minimize losses due to shading. Among all topologies, Magic Square (MS) topology performs in a better way considering all the factors like shading, output power, Mismatch Losses, Fill Factor and efficiency. A MS is a special topology in which numbers are arranged in such a pattern that by adding every row, every column and diagonal gives the same number. This same number is known as Magic Sum. The number of rows and columns can be identified by the order of MS. In general, order of MS is n with n rows and columns. The electrical connection remains the same while panels get physically relocated. The comparison of all configurations is shown by various charts. Different configurations power, Mismatch Losses, Fill Factor and efficiency have been obtained and verified using Matlab/Simulink.

The cost of PV array varies across the globe. All configurations would be differ in terms of cost due to different wiring pattern. In Series Parallel (SP) configuration, PV modules are directly connected to each other like PV module of first row first column is connected in parallel with the adjacent module of first row second column resulting less wiring cost while in MS, PV module of first row first column is connected in parallel with the PV module of third row second column which is located at some distance so this irregular sequence of pv modules would lead to more wiring cost. Thus, on the basis of wiring, MS cost increases 4% to 7% of total cost with respect to SP. Even though this high cost can be compensated as high efficiency of MS pattern. However, this paper is not analyzed based on cost factor.

This work contains bypass diode connected in parallel with PV panel. The use of bypass diode prevents hot spot caused by shading on panel. Due to shading, current gets limited and its path got blocked. Bypass diode mitigates this by allowing current to bypass the shaded part. However, if bypass diode is absent, effect of shading will be more which leads to more losses and less efficiency.

TABLE 1. Comparison of existing literatures with present work.

Reference	Existing works	Present work
[14]	Conventional and hybrid topologies are analyzed and simulated to enhance maximum power and reduce Mismatch Losses. No work is done on Magic Square topology and efficiency assessment.	Magic Square topology is compared with other configurations and efficiency assessment is accomplished.
[15]	The comparative analysis is done among TCT, irradiance equalization technique, and proposed method, that is, direct power evaluation-based re-configuration strategy to find the global optimal configuration. This method unable to find the optimal configuration fast in case of larger PV arrays and assessment is done only on basis of output power.	Accomplishment of assessment on basis of output power, Fill Factor, Mismatch Losses and efficiency.
[16]	Describe the procedure for obtaining the optimized topology, that is, the change of the series-parallel connection among the panels of which it is made up for achieving high performance. No other configuration except Series Parallel is taken into account for analysis.	Analysis is done on Total Cross Tied, Physical Relocation of Module with Fixed Electrical Connections, SuDoKu and Magic Square.
[18]	It compares TCT with physical relocation and fixed column position of modules with fixed electrical connection (PRFCPM-FEC) to enhance the performance based on output power and Mismatch Losses under shading conditions	SuDoKu and Magic Square topology are also analyzed. Fill Factor and efficiency assessment is accomplished.
[26]	This paper gives optimal SuDoKu topology performance under various partial shading patterns based on Fill Factor, efficiency, Mismatch Losses and global maximum power peak by using Matlab/Simulink. Analysis is done on TCT, SuDoKu and optimal SuDoKu topology.	Analysis is also done on Physical Relocation of Module with Fixed Electrical Connections and Magic Square.
[28]	This Paper investigated modified SuDoKu topology in comparison with TCT. Analysis is done on TCT, SuDoKu and modified SuDoKu topology.	Analysis is also done on Physical Relocation of Module with Fixed Electrical Connections and Magic Square.
[29]	This paper compares TCT, SuDoKu and Magic Square view topology on basis of output power.	Accomplishment of assessment on basis of output power, Fill Factor, Mismatch Losses and efficiency.
[30-32]	Comparison and analysis is done between Magic Square and reconfigured TCT. Efficiency assessment is not accomplished.	Comparative analysis is done on Total Cross Tied, Physical Relocation of Module with Fixed Electrical Connections, SuDoKu and Magic Square. Efficiency assessment is accomplished.

III. VARIOUS CONFIGURATIONS BEHAVIOUR UNDER DIFFERENT SHADING PATTERNS

Less amount of shading can adversely affect solar PV system efficiency. For analysis, various configurations are subjected to various shading patterns. These patterns are dependent on total columns which are shaded and total panels which are shaded per column. The types of patterns are as follows: Long Narrow (LnN), Short Narrow (ShN), Long Wide (LnW), Short Wide (ShW) as shown in Fig. 1. Diagonal pattern is also employed, and all these patterns are considered for 5×5 configurations.

A. SERIES-PARALLEL (SP)

By implementing just series or parallel configuration itself, it is not possible to increase voltage and current range

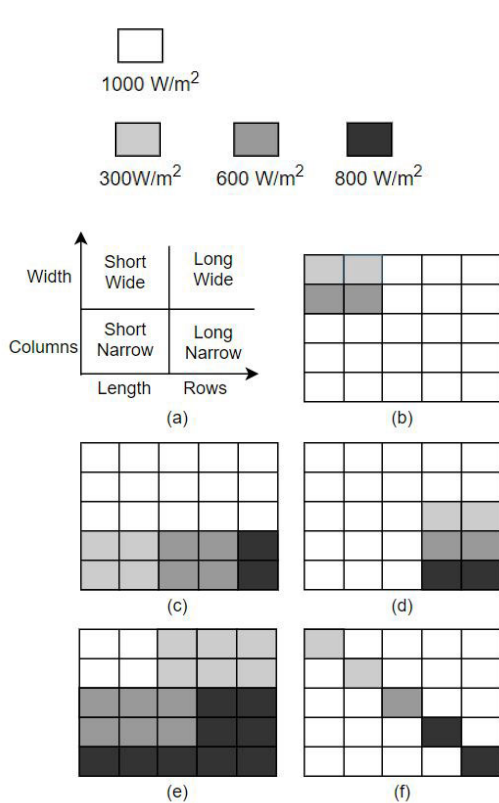


FIGURE 1. (a) Types of shading patterns where shaded blocks represents irradiation 300 W/m^2 , 600 W/m^2 , 800 W/m^2 and unshaded blocks represents irradiation 1000 W/m^2 . (b) Short Narrow pattern (ShN). (c) Short Wide Pattern (ShW). (d) Long Narrow Pattern (LnN). (e) Long Wide pattern (LnW). (f) Diagonal pattern.

simultaneously. Thus, their combination SP is required which includes merits of less cost and electrical losses along with the reliability of the configuration. Five modules are connected in series forming string and five of these strings are connected in parallel to obtain SP configuration as shown in Fig. 2. Multiple peaks are obtained when the panels are in series while for modules which are attached in parallel configuration; single pinnacle is formed in partial shading condition. Series Parallel is most widely used configuration and very easy to implement. The series along with parallel enhance overall output of PV system but it has a drawback that it cannot perform well under partial shading condition.

B. TOTAL CROSS TIED (TCT)

TCT is basically extracted from SP topology and somewhat difficult to implement as compared to SP. It has an additional feature of crossly connected Rows and columns such that total voltage and total current is equal across all Rows and all columns respectively as shown in Fig. 3. The figure also shows all shading conditions at different irradiation's. This scheme works better than SP in shading condition and reduces Mismatch Losses but it has a problem that the number of ties is more which increases cable losses.

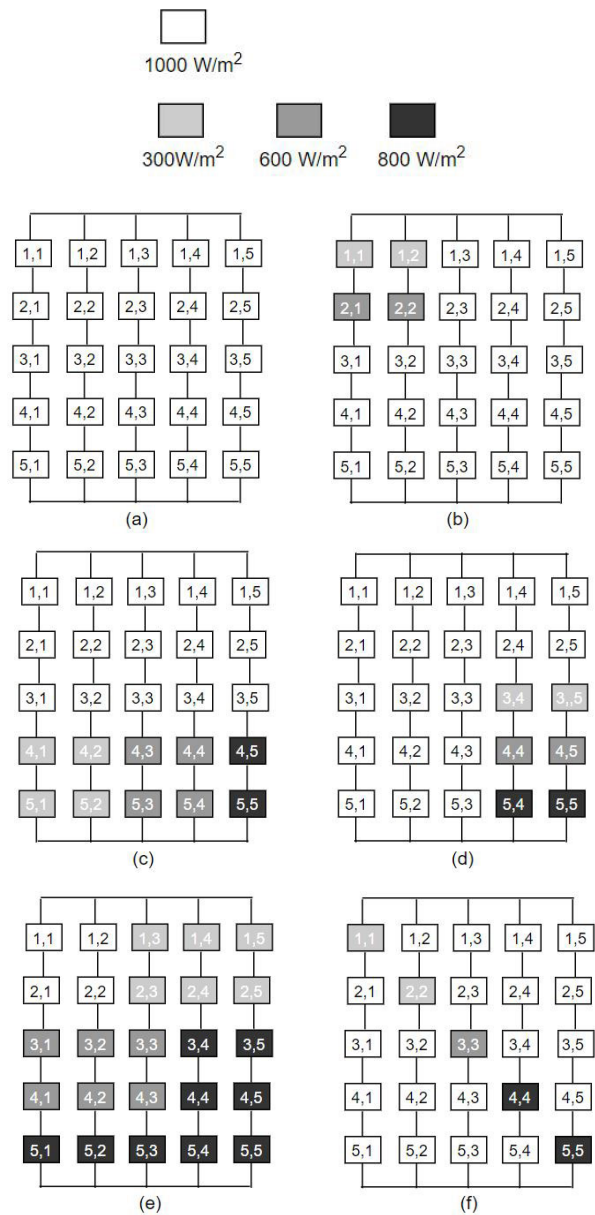


FIGURE 2. (a) Series-Parallel connection where shaded blocks represents irradiation 300 W/m^2 , 600 W/m^2 , 800 W/m^2 and unshaded blocks represents irradiation 1000 W/m^2 . (b) Short Narrow pattern (ShN). (c) Short Wide Pattern (ShW). (d) Long Narrow Pattern (LnN). (e) Long Wide pattern (LnW). (f) Diagonal pattern.

1) BRIDGE LINKED (BL)

Bridge rectifier structure is the Bridge link configuration. It is obtained from TCT with a benefit of lesser number of ties, less wiring installation time and low cable losses but it adversely affects overall voltage and current under shading conditions. The ties pattern which connects PV modules can be seen by Fig. 4.

2) HONEY COMB (HC)

This structure is obtained from idea of Total Cross Tied based on honeycomb structure. The ties connecting pattern

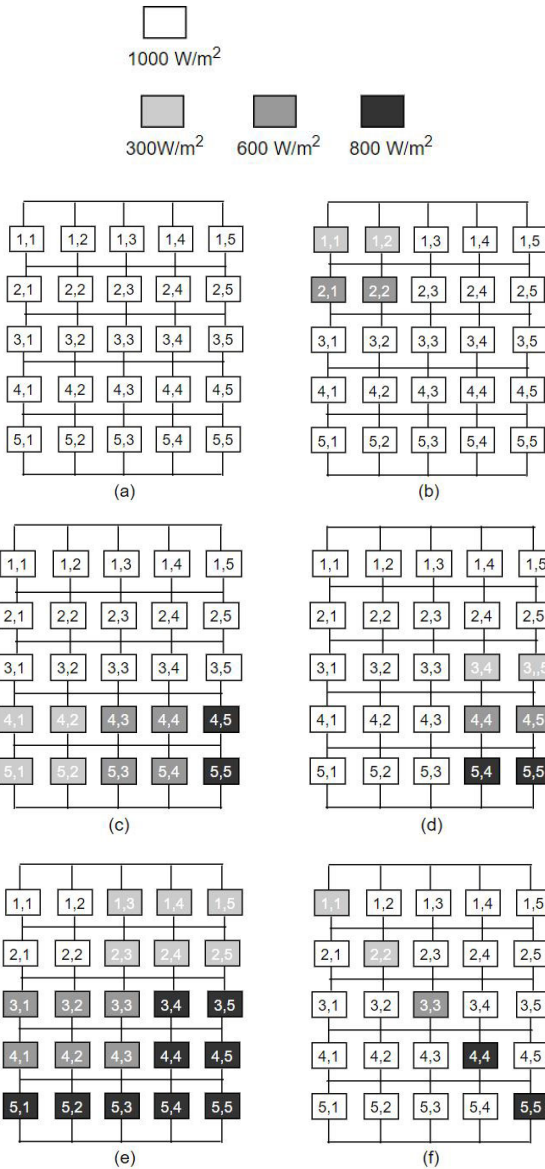


FIGURE 3. (a) TCT connection where shaded blocks represents irradiation 300 W/m^2 , 600 W/m^2 , 800 W/m^2 and unshaded blocks represents irradiation 1000 W/m^2 . (b) Short Narrow pattern (ShN). (c) Short Wide Pattern (ShW). (d) Long Narrow Pattern (LnN). (e) Long Wide pattern (LnW). (f) Diagonal pattern.

is somewhat different from BL as shown in Fig. 4. In this configuration, output power losses can be minimized but it has a limitation that it cannot reduce power losses under all shading conditions.

C. PHYSICAL RELOCATION OF MODULE WITH FIXED ELECTRICAL CONNECTIONS (PRM-FEC) SHADE DISPERSION METHOD

This shade dispersion method has advantage of spreading of shaded part in order to avoid more shading in a same row or same column. In this method, the electrical connections remain unaltered with the relocation of solar PV

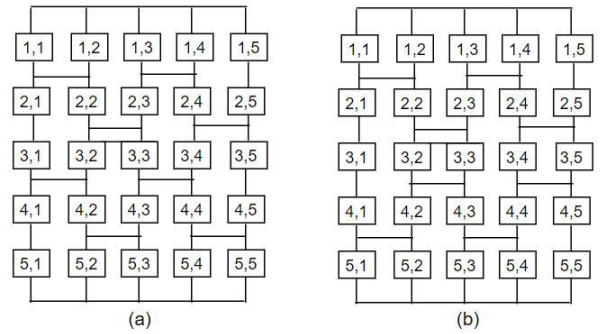


FIGURE 4. Types of TCT connection. (a) Bridge Link Structure (BL). (b) Honeycomb Structure (HC).

module. The shading elements with shading transitions differs from TCT and SP as shown in Fig. 5. It has a demerit that it is difficult to implement due to physical relocation and also its wire cost enhances. The PRM-FEC pattern obtained from TCT pattern which involves odd row algorithm. To achieve the specific result, redundancy in array for a particular row or particular column is not considered. This procedure used for preparing PRM-FEC pattern employs equations (1)-(25) which provides the elements of each row in 5×5 PV matrix.

1. The first column will be in usual manner as given in equation (1)-(5), where R represents row.

$$\begin{aligned}
 R1 &= 1, 1 & (1) \\
 R2 &= 2, 1 & (2) \\
 R3 &= 3, 1 & (3) \\
 R4 &= 4, 1 & (4) \\
 R5 &= 5, 1 & (5)
 \end{aligned}$$

2. For second column, elements of rows are arranged by summation of h and i, where $h = r/2$, $i = 1, 2, 3, 4, 5$ and $r =$ total number of rows. If $h + i > r$ then $h + i$ is replaced by $h + i - r$ as given in equation (6)-(10).

$$\begin{aligned}
 R1 &= h + i - r, 3 = 2, 3 & (6) \\
 R2 &= h + i - r, 3 = 3, 3 & (7) \\
 R3 &= h + i, 3 = 4, 3 & (8) \\
 R4 &= h + i, 3 = 5, 3 & (9) \\
 R5 &= h + i, 3 = 1, 3 & (10)
 \end{aligned}$$

3. For third column, elements of Rows are obtained by summation of h and modified i ($i = 4, 5, 1, 2, 3$) in step 2. If $h+i > r$ then $h+i$ is replaced by $h+i-r$ as given in equation (11)-(15).

$$\begin{aligned}
 R1 &= h + i - r, 3 = 2, 3 & (11) \\
 R2 &= h + i - r, 3 = 3, 3 & (12) \\
 R3 &= h + i, 3 = 4, 3 & (13) \\
 R4 &= h + i, 3 = 5, 3 & (14) \\
 R5 &= h + i, 3 = 1, 3 & (15)
 \end{aligned}$$

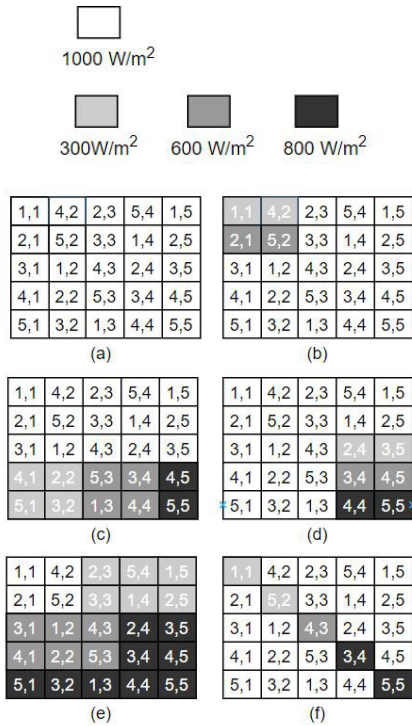


FIGURE 5. (a) PRM-FEC pattern where shaded blocks represents irradiation 300 W/m², 600 W/m², 800 W/m² and unshaded blocks represents irradiation 1000 W/m². (b) Short Narrow pattern (ShN). (c) Short Wide Pattern (ShW). (d) Long Narrow Pattern (LnN). (e) Long Wide pattern (LnW). (f) Diagonal pattern.

4. Similarly for fourth column as expressed in equations (16)-(20).

$$R1 = 5, 4 \tag{16}$$

$$R2 = 1, 4 \tag{17}$$

$$R3 = 2, 4 \tag{18}$$

$$R4 = 3, 4 \tag{19}$$

$$R5 = 4, 4 \tag{20}$$

5. For fifth column as expressed in equation (21)-(25).

$$R1 = 1, 5 \tag{21}$$

$$R2 = 2, 5 \tag{22}$$

$$R3 = 3, 5 \tag{23}$$

$$R4 = 4, 5 \tag{24}$$

$$R5 = 5, 5 \tag{25}$$

D. SuDoKu

This represents logical riddle pattern which is a difficult to implement as compared to previous configurations. A 5 × 5 TCT matrix is considered for SuDoKu configuration whose first digit represent row number and second digit represent column number as shown in Fig. 6. Regarding performance, this pattern is good even under shading conditions. In this configuration, the modules relocation occurs irrespective of

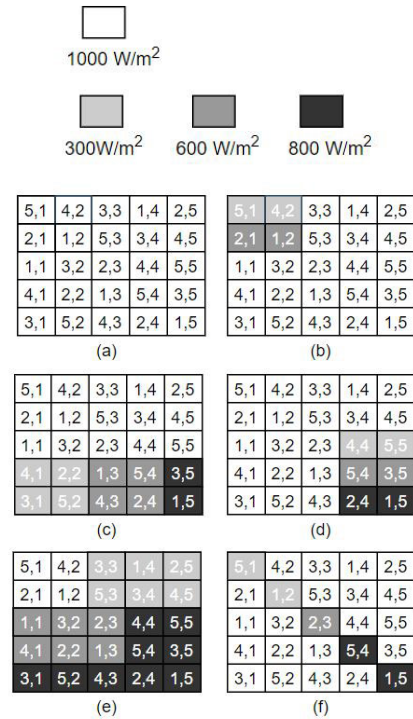


FIGURE 6. (a) SuDoKu pattern where shaded blocks represents irradiation 300 W/m², 600 W/m², 800 W/m² and unshaded blocks represents irradiation 1000 W/m². (b) Short Narrow pattern (ShN). (c) Short Wide Pattern (ShW). (d) Long Narrow Pattern (LnN). (e) Long Wide pattern (LnW). (f) Diagonal pattern.

electrical connections. The physical relocation of modules is limited by increase in the cost of wires.

E. MAGIC SQUARE (MS)

A MS has special number arranged such that by adding every R, every column and diagonals gives same number. A 5 × 5 square matrix is considered for MS pattern where the magic number is 15. The first and second digit represents row and column respectively. In this configuration, electrical connections remain the same while panels get physically relocated which is shown in Fig. 7. This topology performs good among other configurations under shading transitions but due to relocation, its implementation is a difficult task to achieve and its price enhances. The equations (26)-(50) indicates each row elements of MS configuration.

The following steps are taken to produce 5 × 5 MS matrix:
1. The first column will be in usual manner as given in equation (26)-(30), where R represents Row.

$$R1 = 1, 1 \tag{26}$$

$$R2 = 2, 1 \tag{27}$$

$$R3 = 3, 1 \tag{28}$$

$$R4 = 4, 1 \tag{29}$$

$$R5 = 5, 1 \tag{30}$$

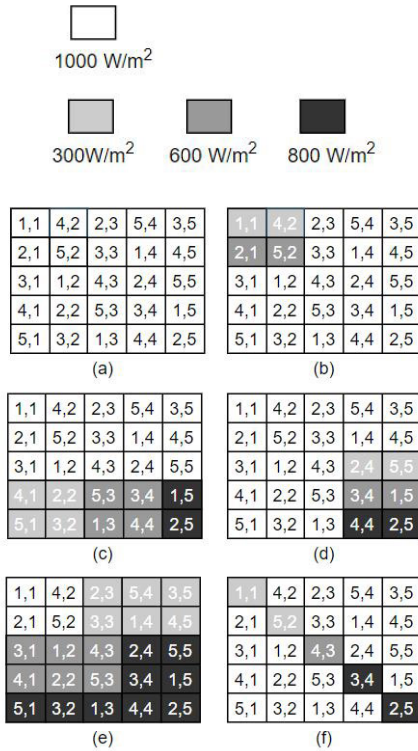


FIGURE 7. (a) MS pattern where shaded blocks represents irradiation 300 W/m², 600 W/m², 800 W/m² and unshaded blocks represents irradiation 1000 W/m². (b) Short Narrow pattern (ShN). (c) Short Wide Pattern (ShW). (d) Long Narrow Pattern (LnN). (e) Long Wide pattern (LnW). (f) Diagonal pattern.

2. For second column, elements of Rows are arranged by summation of h and i, where h = r/2, i = 1, 2, 3, 4, 5 and r = total number of Rows. If h + i > r then h + i is replaced by h + i - r as given in equation (31)-(35).

$$R1 = h + i, 2 = 4, 2 \tag{31}$$

$$R2 = h + i, 2 = 5, 2 \tag{32}$$

$$R3 = h + i - r, 2 = 1, 2 \tag{33}$$

$$R4 = h + i - r, 2 = 2, 2 \tag{34}$$

$$R5 = h + i - r, 2 = 3, 2 \tag{35}$$

3. For third column, elements of rows are obtained by summation of h and modified i (i = 4, 5, 1, 2, 3) in step 2. If h + i > r then h + i is replaced by h + i - r as given in equation (36)-(40).

$$R1 = h + i - r, 3 = 2, 3 \tag{36}$$

$$R2 = h + i - r, 3 = 3, 3 \tag{37}$$

$$R3 = h + i, 3 = 4, 3 \tag{38}$$

$$R4 = h + i, 3 = 5, 3 \tag{39}$$

$$R5 = h + i, 3 = 1, 3 \tag{40}$$

4. For fourth column, elements of rows are obtained by summation of h and modified i (i = 2, 3, 4, 5, 1) in step 3.

TABLE 2. PV module specifications.

PV Model	TP 180
Module dimension	1587mmx790mmx50mm
Module weight	16kg
Pmax	180W
VMPP	35.8V
IMPP	5.03A
Voc	43.6V
Is	5.48A
Number of cells	72

If h + i > r then h + i is replaced by h + i - r as given in equation (41)-(45).

$$R1 = h + i, 4 = 5, 4 \tag{41}$$

$$R2 = h + i - r, 4 = 1, 4 \tag{42}$$

$$R3 = h + i - r, 4 = 2, 4 \tag{43}$$

$$R4 = h + i - r, 4 = 3, 4 \tag{44}$$

$$R5 = h + i, 4 = 4, 4 \tag{45}$$

5. For fifth column, elements of rows are obtained by summation of h and modified i (i = 5, 1, 2, 3, 4) in step 4. If h + i > r then h + i is replaced by h + i - r as given in equation (46)-(50).

$$R1 = h + i - r, 5 = 3, 5 \tag{46}$$

$$R2 = h + i, 5 = 4, 5 \tag{47}$$

$$R3 = h + i, 5 = 5, 5 \tag{48}$$

$$R4 = h + i - r, 5 = 1, 5 \tag{49}$$

$$R5 = h + i - r, 5 = 2, 5 \tag{50}$$

IV. PV MODULE MODELING

The solar array consists of five modules in the series building a cord and these five cords are joined as in parallel connection. Total 25 modules formed a 5 x 5 matrix. The total power capacity of array is 4.5kW. Table 2 provides information regarding PV module.

The equations (51)-(55) are used to describe the behaviour and control of PV characteristics. These equations plays a vital role in forming a single PV module and also providing current vs voltage as well as power vs voltage characteristics. The photocurrent Ip, saturation current Io, reverse saturation current Ir and shunt current Ish are used to find output current I of PV system.

$$Ip = [Is + Ks.(To - 298)].IRD/1000 \tag{51}$$

$$Io = Ir.(To/Tn)^3.exp([Q.Eg0.(1/Tn - 1/T)])/(D.Kb) \tag{52}$$

$$Ir = Is/(exp((Q.Voc)/(D.N.Kb.To))) - 1 \tag{53}$$

$$Ish = ((V + I.Rse)/Rsh) \tag{54}$$

$$I = Ip - Io.[exp((Q.V + Q.I.Rse)/((D.Kb.N.To)) - 1] - Ish \tag{55}$$

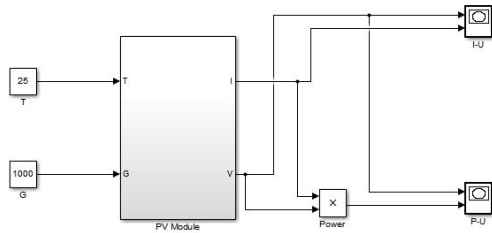


FIGURE 8. Simulated circuit of PV Module.

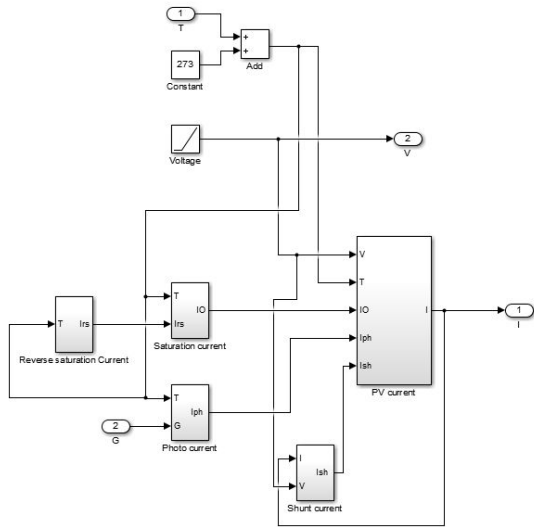


FIGURE 9. Subsystem of PV Module.

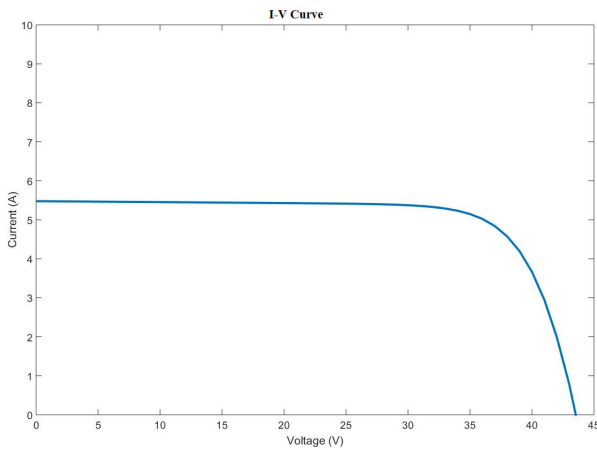


FIGURE 10. Simulated I-V graph of Photovoltaic panel.

The PV module has been drawn in simulink and its simulated circuit is shown in figure Fig. 8. The PV module is a subsystem given in figure Fig. 9 formed by the combination of different subsystems namely saturation current subsystem, reverse saturation current subsystem, photo current subsystem, shunt current subsystem and PV current subsystem. A graph of current Vs voltage and power Vs voltage of PV module at 25°C temperature and 1000 W/m² IRD is shown by figure Fig. 10 and Fig. 11.

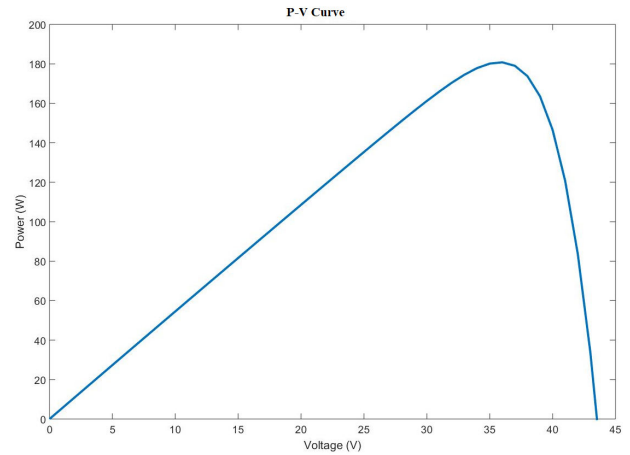


FIGURE 11. Simulated P-V graph of Photovoltaic panel.

V. ANALYSIS OF DIFFERENT CONFIGURATIONS UNDER DIFFERENT SHADING PATTERNS

Five types of shading patterns- ShN, ShW, LnN, LnW and diagonal are considered for analyzing different 5 × 5 configurations. Four irradiation levels are considered, the shaded part receives 300 W/m², 600 W/m², 800 W/m² and unshaded part receives 1000 W/m². For ShN pattern in TCT Configuration, two modules of R1 and R2 receives 300 W/m² and 600 W/m² respectively, rest of the panels receives 1000 W/m² while all modules of R3, R4 and R5 receives 1000 W/m² as given in equations (56)-(59).

$$IR = 5 * (IRD/ISTC)Im \tag{56}$$

$$IR1 = 2 * (300/1000)Im + 3 * (1000/1000)Im = 3.6Im \tag{57}$$

$$IR2 = 2 * (600/1000)Im + 3 * (1000/1000)Im = 4.2Im \tag{58}$$

$$IR3 = IR4 = IR5 = 5 * (1000/1000)Im = 5Im \tag{59}$$

Similarly, row currents are calculated in terms of module current for other configurations such as PRMFEC, SuDoKu and MS. For ShW, LnN, LnW and diagonal pattern, four irradiation are considered - 300 W/m², 600 W/m², 800 W/m² and 1000 W/m². All the row currents calculated can be refer to appendix table 14 which provides the comparison of power, current and voltage between various configurations under different shading patterns.

VI. SIMULATION RESULTS

To attain the performance of various configurations of a 5 × 5 Photovoltaic system, it is subjected to various shading patterns. Here, it is considered that the panels which are not shaded get 1000 W/m² irradiation and the panels which are shaded get 300 W/m², 600 W/m², 800 W/m² irradiation.

Table 3 represents comparison between simulated values of power, current and voltage of various topologies under Short Narrow shading pattern. The SuDoKu and MS performance

TABLE 3. Comparison of various configurations under Short Narrow pattern.

Configurations	I (amp)	V (Volt)	P (Watt)
TCT	22.98	114.9	2641
PRM-FEC	23.32	116.6	2719
SuDoKu	23.49	117.5	2760
MS	23.49	117.5	2760

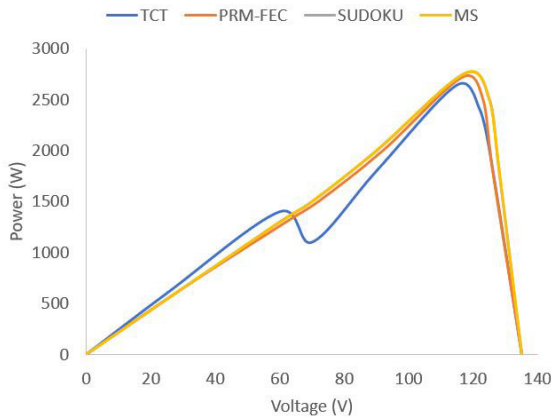


FIGURE 12. P-V graph of various configurations under ShN shading patterns.

TABLE 4. Comparison of various configurations under Short Wide pattern.

Configurations	I (amp)	V (Volt)	P (Watt)
TCT	20.12	100.6	2025
PRM-FEC	21.22	106.1	2251
SuDoKu	21.51	110.2	2370
MS	22.58	112.9	2550

TABLE 5. Comparison of various configurations under Long Narrow pattern.

Configurations	I (amp)	V (Volt)	P (Watt)
TCT	22.96	114.8	2636
PRM-FEC	23.42	117.1	2743
SuDoKu	23.44	117.2	2747
MS	23.99	119.9	2877

is better than TCT and PRM-FEC configurations. The maximum power obtained in this pattern is 2760 W. Fig. 12 gives the effect of changing voltage on output power.

It has been observed by table 4 that under Short Wide pattern MS performance is better than other configurations. The output power of 2550 W is obtained in MS. Fig. 13 shows power vs voltage graph of different configurations.

By table 5, simulated values are compared of various topologies of under Long Narrow pattern. The MS topology provides better performance than other configurations. The power voltage characteristics shown by Fig. 14 indicates the performance of different configurations.

Table 6 represents comparison between simulated values of P,V and I of various topologies under Long Wide pattern. It can be seen that MS topology gives highest output power

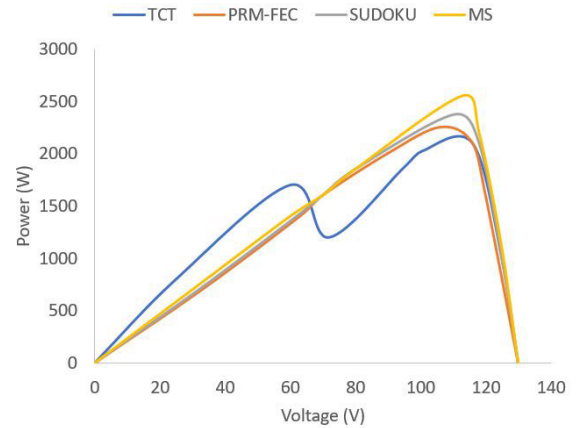


FIGURE 13. P-V graph of various configurations under ShW shading patterns.

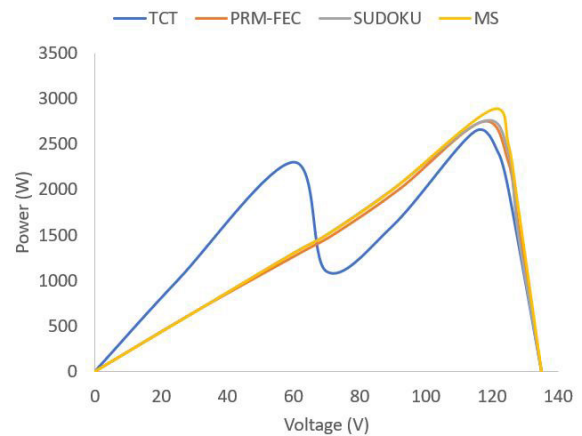


FIGURE 14. P-V graph of various configurations under LnN shading patterns.

TABLE 6. Comparison of various configurations under Long Wide pattern.

Configurations	I (amp)	V (Volt)	P (Watt)
TCT	17.93	89.63	1607
PRM-FEC	17.95	89.72	1612
SuDoKu	18.24	91.21	1644
MS	18.54	92.72	1719

TABLE 7. Comparison of various configurations under diagonal pattern.

Configurations	I (amp)	V (Volt)	P (Watt)
TCT	23.5	117.5	2761
PRM-FEC	21.82	111.5	2433
SuDoKu	22.46	112.3	2522
MS	23.5	117.5	2761

of 1719 W among other configurations. Fig. 15 gives variation in power as per voltage under Long Wide shade.

Table 7 analyzes simulated values of P,V and I of various topologies under diagonal pattern. It is shown that TCT and MS topology performance is better than other configurations. The P-U curve under this pattern is given by Fig. 16.

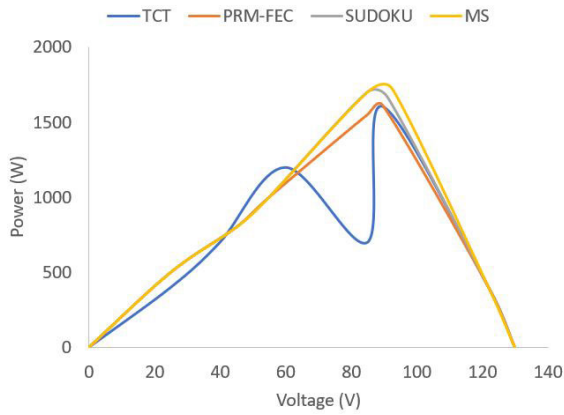


FIGURE 15. P-V graph of various configurations under LnW shading patterns.

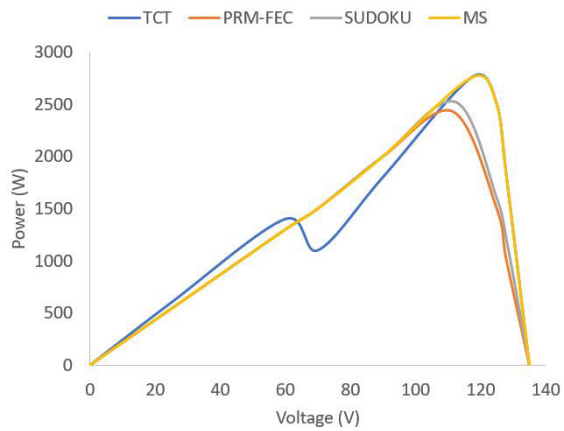


FIGURE 16. P-V graph of various configurations under diagonal shading patterns.

TABLE 8. Power enhancement of MS with respect to TCT, PRM-FEC and SuDoKu.

Shading Patterns	TCT (%)	PRM-FEC (%)	SuDoKu (%)
ShN	4.5	1.5	0
ShW	25.9	13.3	7.6
LnN	9.1	4.9	4.7
LnW	7.0	6.6	3.3
Diagonal	0	13.5	9.5

The power, voltage and current comparison of different configurations are shown in figures Fig. 17-19. MS topology provides maximum power in all the patterns. The causes of these results is shading distribution among all modules. In some cases such as MS, shading dispersed in non uniform pattern so most of the panels are in active mode, therefore, MS achieve highest output power and maximum efficiency among all topologies. The power enhancement of MS with respect to other topologies are shown via table 8. It is seen that SuDoKu is comparable to MS under ShN pattern and TCT is comparable to MS under diagonal pattern.

The ML are the effect of Photovoltaic panels interconnections which do not share same conditions. The mathematical

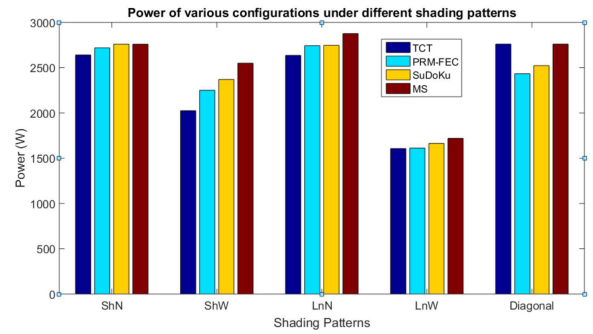


FIGURE 17. Power of various configurations under different shading patterns.

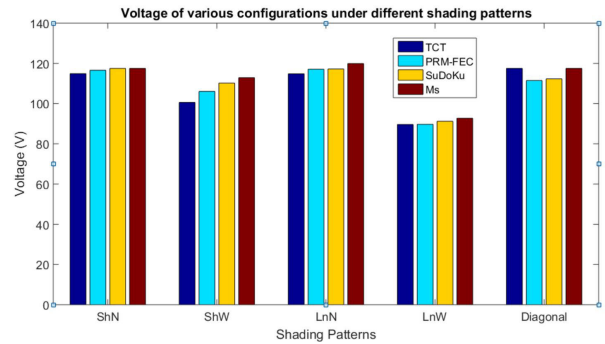


FIGURE 18. Voltage of various configurations under different shading patterns.

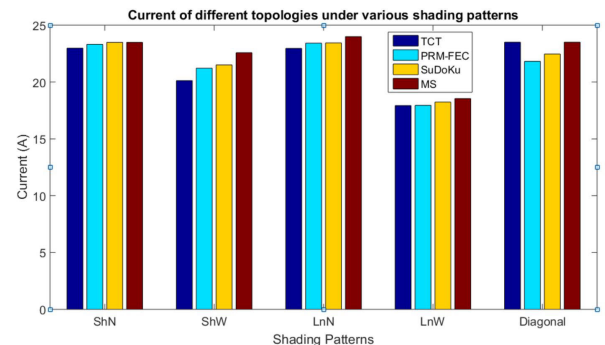


FIGURE 19. Current of different topologies under various shading patterns.

expression of mismatch power loss is given in equation (60).

$$\text{Mismatch powerloss} = \text{GMPPSTC} - \text{GMPPPS} \quad (60)$$

where, GMPP represents global maximum power point, GMPPSTC denotes global maximum power point at standard test condition, GMPPPS means global maximum power point at partial shading, and PS indicates partial shading.

The FF represents the degree of PV array Quality. Mathematically it is represented as given in equation (61).

$$FF = (\text{Max. Power at PS}) / (\text{Rated power of PV array}) \quad (61)$$

TABLE 9. Mismatch Losses, FF and Efficiency comparison of various configurations under Short Narrow pattern.

Configurations	Mismatch Losses (W)	FF	Efficiency (%)
TCT	1008	0.442	9.24
PRM-FEC	930	0.455	9.51
SuDoKu	889	0.462	9.66
MS	889	0.462	9.66

TABLE 10. Mismatch Losses, FF and Efficiency comparison of various configurations under Short Wide pattern.

Configurations	Mismatch Losses (W)	FF	Efficiency (%)
TCT	1624	0.339	8.00
PRM-FEC	1398	0.376	8.89
SuDoKu	1279	0.396	9.36
MS	1099	0.426	9.55

TABLE 11. Mismatch Losses, FF and Efficiency comparison of various configurations under Long Narrow pattern.

Configurations	Mismatch Losses (W)	FF	Efficiency (%)
TCT	1013	0.441	9.39
PRM-FEC	906	0.459	9.77
SuDoKu	902	0.460	9.78
MS	772	0.481	10.24

TABLE 12. Mismatch Losses, FF and Efficiency comparison of various configurations under Long Wide pattern.

Configurations	Mismatch Losses (W)	FF	Efficiency (%)
TCT	2042	0.269	7.72
PRM-FEC	2037	0.270	7.75
SuDoKu	1985	0.278	8.00
MS	1930	0.287	8.26

The efficiency of Photovoltaic array can be calculated using the expression as given in equation (62).

$$Efficiency = (Max.Power)/(Irradiation * Area of array) \tag{62}$$

Table 9 tabulated Mismatch Losses, FF and efficiency comparison of various configurations under Short Narrow pattern. The highest efficiency is 9.66% which is obtained for two configurations – SuDoKu and MS.

The different configurations under ShW patterns have been shown by table 10 in which the highest efficiency is obtained by MS configurations i.e. 9.55%.

Based on different parameters, it has been analyzed that MS configuration under LnN patterns shown by table 11 provides highest efficiency which is 10.24%.

The MS configuration under LnW pattern gives highest efficiency of 8.26% while other configurations gives lowest efficiency as shown by table 12.

Different parameters based configurations under diagonal shading patterns have been shown by table 13. The highest efficiency is 9.41% which is obtained for two configurations– TCT and MS.

The ML, FF and efficiency comparison of different configurations are shown by figures Fig. 20-22. MS topology

TABLE 13. Mismatch Losses, FF and Efficiency comparison of various configurations diagonal pattern.

Configurations	Mismatch Losses(W)	FF	Efficiency(%)
TCT	888	0.462	9.41
PRM-FEC	1216	0.407	8.30
SuDoKu	1127	0.422	8.60
MS	888	0.462	9.41

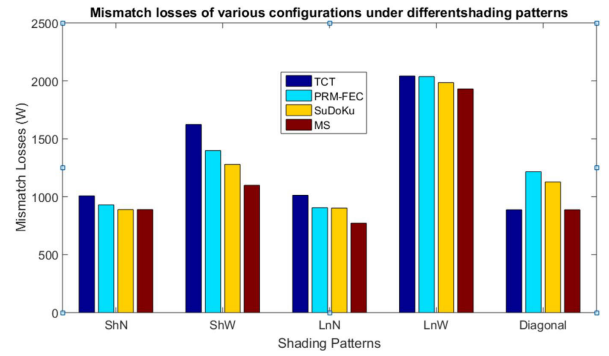


FIGURE 20. Mismatch Losses of various configurations under different shading patterns.

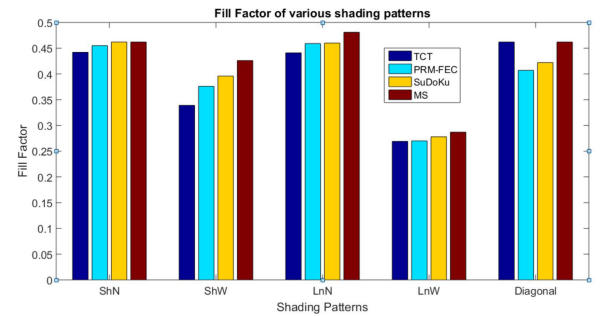


FIGURE 21. Fill Factor of various shading patterns.

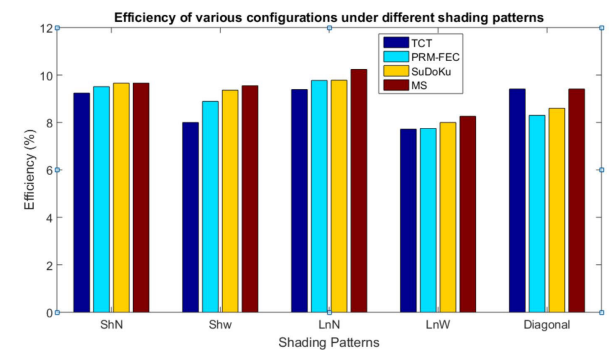


FIGURE 22. Efficiency of various configurations under different shading patterns.

provides maximum efficiency in all the patterns. SuDoKu and TCT configurations along with MS topology are suitable for ShN and diagonal patterns while for rest of the patterns, MS is more suitable.

VII. CONCLUSION

The performance of 5 × 5 array based on different topologies such as TCT, PRM-FEC, SuDoKu and MS are studied and analyzed in detail using MATLAB/SIMULINK.

TABLE 14. Power, current and voltage comparison of various topologies.

Shading Patterns	TCT	PRM-FEC	SuDoKu	MS
SN	IR1 = 3.6Im, 1Vm, P = 3.60 Vm Im	IR1 = 4.3Im, 1Vm, P = 4.30 Vm Im	IR1 = 4.6Im, 1Vm, P = 4.60 Vm Im	IR1 = 4.3Im, 1Vm, P = 4.30 Vm Im
	IR2 = 4.2Im, 2Vm, P = 8.40 Vm Im	IR2 = 4.6Im, 2Vm, P = 9.20 Vm Im	IR2 = 4.6Im, 2Vm, P = 9.20 Vm Im	IR2 = 4.6Im, 2Vm, P = 9.20 Vm Im
	IR3 = 5.0Im, 3Vm, P = 15.0 Vm Im	IR3 = 5.0Im, 3Vm, P = 15.0 Vm Im	IR3 = 5.0Im, 3Vm, P = 15.0 Vm Im	IR3 = 5.0Im, 3Vm, P = 15.0 Vm Im
	IR4 = 5.0Im, 4Vm, P = 20.0 Vm Im	IR4 = 4.3Im, 4Vm, P = 17.2 Vm Im	IR4 = 4.3Im, 4Vm, P = 17.2 Vm Im	IR4 = 4.3Im, 4Vm, P = 17.2 Vm Im
	IR5 = 5.0Im, 5Vm, P = 25.0 Vm Im	IR5 = 4.6Im, 5Vm, P = 23.0 Vm Im	IR5 = 4.3Im, 5Vm, P = 21.5 Vm Im	IR5 = 4.6Im, 5Vm, P = 23.0 Vm Im
SW	IR1 = 5.0Im, 1Vm, P = 5.00 Vm Im	IR1 = 4.6Im, 1Vm, P = 4.60 Vm Im	IR1 = 4.4Im, 1Vm, P = 4.40 Vm Im	IR1 = 4.4Im, 1Vm, P = 4.40 Vm Im
	IR2 = 5.0Im, 2Vm, P = 10.0 Vm Im	IR2 = 4.3Im, 2Vm, P = 8.60 Vm Im	IR2 = 3.9Im, 2Vm, P = 7.80 Vm Im	IR2 = 4.1Im, 2Vm, P = 8.20 Vm Im
	IR3 = 5.0Im, 3Vm, P = 15.0 Vm Im	IR3 = 3.9Im, 3Vm, P = 11.7 Vm Im	IR3 = 4.1Im, 3Vm, P = 12.3 Vm Im	IR3 = 3.9Im, 3Vm, P = 11.7 Vm Im
	IR4 = 2.6Im, 4Vm, P = 10.4 Vm Im	IR4 = 3.7Im, 4Vm, P = 14.8 Vm Im	IR4 = 3.9Im, 4Vm, P = 15.6 Vm Im	IR4 = 3.9Im, 4Vm, P = 15.6 Vm Im
	IR5 = 2.6Im, 5Vm, P = 13.0 Vm Im	IR5 = 3.7Im, 5Vm, P = 18.5 Vm Im	IR5 = 3.9Im, 5Vm, P = 19.5 Vm Im	IR5 = 3.9Im, 5Vm, P = 19.5 Vm Im
LN	IR1 = 5.0Im, 1Vm, P = 5.00 Vm Im	IR1 = 5.0Im, 1Vm, P = 15.0 Vm Im	IR1 = 4.8Im, 1Vm, P = 4.80 Vm Im	IR1 = 4.6Im, 1Vm, P = 4.60 Vm Im
	IR2 = 5.0Im, 2Vm, P = 10.0 Vm Im	IR2 = 4.3Im, 2Vm, P = 8.6 Vm Im	IR2 = 4.8Im, 2Vm, P = 9.60 Vm Im	IR2 = 4.1Im, 2Vm, P = 8.20 Vm Im
	IR3 = 3.6Im, 3Vm, P = 10.8 Vm Im	IR3 = 3.9Im, 3Vm, P = 11.7 Vm Im	IR3 = 4.6Im, 3Vm, P = 13.8 Vm Im	IR3 = 4.6Im, 3Vm, P = 13.8 Vm Im
	IR4 = 4.2Im, 4Vm, P = 16.8 Vm Im	IR4 = 4.4Im, 4Vm, P = 17.6 Vm Im	IR4 = 4.6Im, 4Vm, P = 18.4 Vm Im	IR4 = 4.8Im, 4Vm, P = 19.2 Vm Im
	IR5 = 4.6Im, 5Vm, P = 23.0 Vm Im	IR5 = 4.8Im, 5Vm, P = 24.0 Vm Im	IR5 = 4.6Im, 5Vm, P = 23.0 Vm Im	IR5 = 4.3Im, 5Vm, P = 21.5 Vm Im
LW	IR1 = 2.9Im, 1Vm, P = 2.90 Vm Im	IR1 = 3.0Im, 1Vm, P = 3.00 Vm Im	IR1 = 3.3Im, 1Vm, P = 3.30 Vm Im	IR1 = 3.5Im, 1Vm, P = 3.50 Vm Im
	IR2 = 2.9Im, 2Vm, P = 5.80 Vm Im	IR2 = 3.0Im, 2Vm, P = 6.00 Vm Im	IR2 = 3.3Im, 2Vm, P = 6.60 Vm Im	IR2 = 3.5Im, 2Vm, P = 7.00 Vm Im
	IR3 = 3.4Im, 3Vm, P = 10.2 Vm Im	IR3 = 3.3Im, 3Vm, P = 9.90 Vm Im	IR3 = 2.8Im, 3Vm, P = 8.40 Vm Im	IR3 = 2.8Im, 3Vm, P = 8.40 Vm Im
	IR4 = 3.4Im, 4Vm, P = 13.6 Vm Im	IR4 = 3.8Im, 4Vm, P = 15.2 Vm Im	IR4 = 3.5Im, 4Vm, P = 14.0 Vm Im	IR4 = 3.3Im, 4Vm, P = 13.2 Vm Im
	IR5 = 4.0Im, 5Vm, P = 20.0 Vm Im	IR5 = 3.5Im, 5Vm, P = 17.5 Vm Im	IR5 = 3.7Im, 5Vm, P = 18.5 Vm Im	IR5 = 3.5Im, 5Vm, P = 17.5 Vm Im
Diagonal	IR1 = 4.3Im, 1Vm, P = 4.30 Vm Im	IR1 = 4.3Im, 1Vm, P = 4.30 Vm Im	IR1 = 4.1Im, 1Vm, P = 4.10 Vm Im	IR1 = 4.3Im, 1Vm, P = 4.30 Vm Im
	IR2 = 4.3Im, 2Vm, P = 8.60 Vm Im	IR2 = 5.0Im, 2Vm, P = 10.0 Vm Im	IR2 = 4.6Im, 2Vm, P = 9.20 Vm Im	IR2 = 4.8Im, 2Vm, P = 9.60 Vm Im
	IR3 = 4.6Im, 3Vm, P = 13.8 Vm Im	IR3 = 4.8Im, 3Vm, P = 14.4 Vm Im	IR3 = 5.0Im, 3Vm, P = 15.0 Vm Im	IR3 = 4.8Im, 3Vm, P = 14.4 Vm Im
	IR4 = 4.8Im, 4Vm, P = 19.2 Vm Im	IR4 = 4.6Im, 4Vm, P = 18.4 Vm Im	IR4 = 5.0Im, 4Vm, P = 20.0 Vm Im	IR4 = 4.6Im, 4Vm, P = 18.4 Vm Im
	IR5 = 4.8Im, 5Vm, P = 24.0 Vm Im	IR5 = 4.1Im, 5Vm, P = 20.5 Vm Im	IR5 = 4.1Im, 5Vm, P = 20.5 Vm Im	IR5 = 4.3Im, 5Vm, P = 21.5 Vm Im

The parameters which are used to measure the performance are current, voltage, Power, ML, FF and efficiency. Table 2 shows that SuDoKu and MS provides better output power of 2760 W than TCT and PRM-FEC under ShN pattern. The MS configuration achieves highest output power of 2550 W, 2877 W and 1719 W under ShW, LnN and LnW pattern respectively as shown in Table 3 to Table 5. TCT and MS performs in the same way to obtain maximum power of 2761 W under diagonal pattern as mentioned in Table 6. It can be seen in Table 7 that MS power enhances maximum of 25.9 % in comparison with TCT under ShW pattern and 13.5 %, 9.5 % with respect to PRM-FEC and SuDoKu respectively under diagonal pattern. The ML is largest in TCT topology which is 1008 W under ShN pattern as inferred in Table 8. Table 11 shows that ML of TCT is 2042 W which is largest among all the topologies under LnW pattern. Table 10 shows that MS has achieved the highest efficiency of 10.24 % among all configurations under LnN pattern. TCT configuration has lowest efficiency of 7.72 % among all configurations under LnW pattern as seen in table 11. The Fill Factor also varies with different shading conditions. FF is lowest under LnW pattern which is 0.269 and highest in LnN pattern which is 0.481. The efficiencies could be different for each configuration under different shading patterns but by analyzing this work, MS method is showing the highest efficiency under all shading patterns.

APPENDIX

(See Table 14)

ACKNOWLEDGMENT

The authors are thankful to the School of Electrical, Electronics and Communication, Galgotias University, for providing

the resources and data used for this study. The authors would like to acknowledge the support of Prince Sultan University for paying the Article Processing Charges (APC) of this publication and for having rendered their technical support. The authors also thank the Clean and Resilient Energy Systems (CARES) Laboratory, Texas A&M University, Galveston, USA, for the technical expertise provided.

REFERENCES

- [1] X. Qing, H. Sun, X. Feng, and C. Y. Chung, "Submodule-based modeling and simulation of a series-parallel photovoltaic array under mismatch conditions," *IEEE J. Photovolt.*, vol. 7, no. 6, pp. 1731–1739, 2017.
- [2] R. P. Vengatesh and S. E. Rajan, "Investigation of the effects of homogeneous and heterogeneous solar irradiations on multicrystal PV module under various configurations," *IET Renew. Power Gener.*, vol. 9, no. 3, pp. 245–254, Apr. 2015.
- [3] A. Mehiri, A.-K. Hamid, and S. Almazrouei, "The effect of shading with different PV array configurations on the grid-connected PV system," in *Proc. Int. Renew. Sustain. Energy Conf. (IRSEC)*, Tangier, Morocco, Dec. 2017, pp. 1–6.
- [4] K. Lappalainen and S. Valkealahti, "Fluctuation of PV array global maximum power point voltage during irradiance transitions caused by clouds," *IET Renew. Power Gener.*, vol. 13, no. 15, pp. 2864–2870, Nov. 2019.
- [5] V. S. Bhadoria, R. K. Pachauri, S. Tiwari, S. P. Jaiswal, and H. H. Alhelou, "Investigation of different BPD placement topologies for shaded modules in a series-parallel configured PV array," *IEEE Access*, vol. 8, pp. 216911–216921, 2020.
- [6] M. Orkisz, "Estimating effects of individual PV panel failures on PV array output," *IEEE Trans. Ind. Appl.*, vol. 54, no. 5, pp. 4825–4832, Sep. 2018.
- [7] L. Caetano, G. Caaixeta, T. Lima, J. Oliveira, R. Ramos, and A. Rodrigo, "Modelling of a multipurpose photovoltaic generator block using ATP-EMTP," *IEEE Latin Amer. Trans.*, vol. 17, no. 02, pp. 203–209, Feb. 2019.
- [8] A. Mäki and S. Valkealahti, "Power losses in long string and parallel-connected short strings of series-connected silicon-based photovoltaic modules due to partial shading conditions," *IEEE Trans. Energy Convers.*, vol. 27, no. 1, pp. 173–183, Mar. 2012.
- [9] F. Iraj, E. Farjah, and T. Ghanbari, "Optimisation method to find the best switch set topology for reconfiguration of Photovoltaic panels," *IET Renew. Power Gener.*, vol. 12, no. 3, pp. 374–379, 2018

- [10] Y. Mochizuki and T. Yachi, "Relationship between power generated and series/parallel solar panel configurations for 3D fibonacci PV modules," in *Proc. IEEE 6th Int. Conf. Renew. Energy Res. Appl. (ICRERA)*, San Diego, CA, USA, Nov. 2017, pp. 126–130.
- [11] Y. Mochizuki and T. Yachi, "Effective series-parallel cell configuration in solar panels for FPM power generation forest," in *Proc. 7th Int. Conf. Renew. Energy Res. Appl. (ICRERA)*, Paris, France, Oct. 2018, pp. 294–300.
- [12] A. Ul-Haq, R. Alammari, A. Iqbal, M. Jalal, and S. Gul, "Computation of power extraction from photovoltaic arrays under various fault conditions," *IEEE Access*, vol. 8, pp. 47619–47639, 2020.
- [13] B. Veerasamy, T. Takeshita, A. Jote, and T. Mekonnen, "Mismatch loss analysis of PV array configurations under partial shading conditions," in *Proc. 7th Int. Conf. Renew. Energy Res. Appl. (ICRERA)*, Paris, France, Oct. 2018, pp. 1162–1167.
- [14] M. Premkumar, U. Subramaniam, T. S. Babu, R. M. Elavarasan, and L. Mihet-Popa, "Evaluation of mathematical model to characterize the performance of conventional and hybrid PV array topologies under static and dynamic shading patterns," *Energies*, vol. 13, no. 12, pp. 1–37, 2020.
- [15] Z. Zhu, M. Hou, L. Ding, G. Zhu, and Z. Jin, "Optimal photovoltaic array dynamic reconfiguration strategy based on direct power evaluation," *IEEE Access*, vol. 8, pp. 210267–210276, 2020.
- [16] M. L. Gutierrez-Orozco, G. Spagnuolo, J. M. Scarpetta-Ramirez, G. Petrone, and C. A. Ramos-Paja, "Optimized configuration of mismatched photovoltaic arrays," *IEEE J. Photovolt.*, vol. 6, no. 5, pp. 1210–1220, Sep. 2016.
- [17] H. S. Sahu, S. K. Nayak, and S. Mishra, "Maximizing the power generation of a partially shaded PV array," *IEEE J. Emerg. Sel. Topics Power Electron.*, vol. 4, no. 2, pp. 626–637, Jun. 2016.
- [18] M. Kumar, "Enhanced solar PV power generation under PSCs using shade dispersion," *IEEE Trans. Electron Devices*, vol. 67, no. 10, pp. 4313–4320, Oct. 2020.
- [19] S. R. Pendem, S. Mikkili, and P. K. Bonthagorla, "PV distributed-MPP tracking: Total-cross-tied configuration of string-integrated-converters to extract the maximum power under various PSCs," *IEEE Syst. J.*, vol. 14, no. 1, pp. 1046–1057, Mar. 2020.
- [20] N. Pragallapati and V. Agarwal, "Distributed PV power extraction based on a modified interleaved SEPIC for nonuniform irradiation conditions," *IEEE J. Photovolt.*, vol. 5, no. 5, pp. 1442–1453, Sep. 2015.
- [21] S. Obukhov, A. Ibrahim, A. A. Z. Diab, A. S. Al-Sumaiti, and R. Aboelsaud, "Optimal performance of dynamic particle swarm optimization based maximum power trackers for stand-alone PV system under partial shading conditions," *IEEE Access*, vol. 8, pp. 20770–20785, 2020.
- [22] O. Khan, W. Xiao, and M. S. E. Moursi, "A new PV system configuration based on submodule integrated converters," *IEEE Trans. Power Electron.*, vol. 32, no. 5, pp. 3278–3284, May 2017.
- [23] J. P. Ram and N. Rajasekar, "A new global maximum power point tracking technique for solar photovoltaic (PV) system under partial shading conditions (PSC)," *Energy*, vol. 118, pp. 512–525, Jan. 2017.
- [24] D. S. Pillai, J. P. Ram, A. M. Y. M. Ghias, M. A. Mahmud, and N. Rajasekar, "An accurate, shade detection-based hybrid maximum power point tracking approach for PV systems," *IEEE Trans. Power Electron.*, vol. 35, no. 6, pp. 6594–6608, Jun. 2020.
- [25] J. P. Ram and N. Rajasekar, "A novel flower pollination based global maximum power point method for solar maximum power point tracking," *IEEE Trans. Power Electron.*, vol. 32, no. 11, pp. 8486–8499, Nov. 2017.
- [26] S. G. Krishna and T. Moger, "Optimal SuDoKu reconfiguration technique for total-cross-tied PV array to increase power output under non-uniform irradiance," *IEEE Trans. Energy Convers.*, vol. 34, no. 4, pp. 1973–1984, Dec. 2019.
- [27] T. S. Babu, J. P. Ram, T. Dragičević, M. Miyatake, F. Blaabjerg, and N. Rajasekar, "Particle swarm optimization based solar PV array reconfiguration of the maximum power extraction under partial shading conditions," *IEEE Trans. Sustain. Energy*, vol. 9, no. 1, pp. 74–85, Jan. 2018.
- [28] K. Rajani and T. Kandipati, "Maximum power enhancement under partial shadings using modified SuDoKu reconfiguration," *CSEE J. Power Energy Syst.*, early access, Jul. 6, 2020, doi: [10.17775/CSEEJPES.2020.01100](https://doi.org/10.17775/CSEEJPES.2020.01100).
- [29] L. E. Iyasaouy, M. Lahbabi, and A. Oumnad, "A novel magic square view topology of a pv system under partial shading condition," in *Proc. Technol. Mater. Renew. Energy, Environ. Sustain. (TMREES)*, Athens, Greece, Sep. 2018, pp. 1182–1190.
- [30] A. S. Yadav, R. K. Pachauri, Y. K. Chauhan, S. Choudhury, and R. Singh, "Performance enhancement of partially shaded PV array using novel shade dispersion effect on magic-square puzzle configuration," *Sol. Energy*, vol. 144, pp. 780–797, Mar. 2017.
- [31] S. M. Samikannu, R. Namani, and S. K. Subramaniam, "Power enhancement of partially shaded PV arrays through shade dispersion using magic square configuration," *J. Renew. Sustain. Energy*, vol. 8, no. 6, Nov. 2016, Art. no. 063503.
- [32] H. N. Suresh and S. Rajanna, "Performance enhancement of hybrid inter-connected solar photovoltaic array using shade dispersion magic square puzzle pattern technique under partial shading conditions," *Sol. Energy*, vol. 194, pp. 602–617, Dec. 2019.
- [33] A. Xenophontos and A. M. Bazzi, "Model-based maximum power curves of solar photovoltaic panels under partial shading conditions," *IEEE J. Photovolt.*, vol. 8, no. 1, pp. 233–238, Jan. 2018.
- [34] R. Ramakrishna, A. Scaglione, V. Vittal, E. Dall'Anese, and A. Bernstein, "A model for joint probabilistic forecast of solar photovoltaic power and outdoor temperature," *IEEE Trans. Signal Process.*, vol. 67, no. 24, pp. 6368–6383, Dec. 2019.
- [35] K. R. McIntosh, M. D. Abbott, B. A. Sudbury, and J. Meydbray, "Mismatch loss in bifacial modules due to nonuniform illumination in 1-D tracking systems," *IEEE J. Photovolt.*, vol. 9, no. 6, pp. 1504–1512, Nov. 2019.
- [36] S. A. Pelaez, C. Deline, S. M. MacAlpine, B. Marion, J. S. Stein, and R. K. Kostuk, "Comparison of bifacial solar irradiance model predictions with field validation," *IEEE J. Photovolt.*, vol. 9, no. 1, pp. 88–92, Jan. 2019.
- [37] D. Berrian, J. Libal, M. Klenk, H. Nussbaumer, and R. Kopecek, "Performance of bifacial PV arrays with fixed tilt and horizontal single-axis tracking: Comparison of simulated and measured data," *IEEE J. Photovolt.*, vol. 9, no. 6, pp. 1583–1589, Nov. 2019.
- [38] L. Cristaldi, M. Faifer, M. Rossi, and F. Ponci, "A simple photovoltaic panel model: Characterization procedure and evaluation of the role of environmental measurements," *IEEE Trans. Instrum. Meas.*, vol. 61, no. 10, pp. 2632–2641, Oct. 2012.
- [39] H. Sangrody, N. Zhou, and Z. Zhang, "Similarity-based models for day-ahead solar PV generation forecasting," *IEEE Access*, vol. 8, pp. 104469–104478, 2020.
- [40] C. W. Hansen and B. H. King, "Determining series resistance for equivalent circuit models of a PV module," *IEEE J. Photovolt.*, vol. 9, no. 2, pp. 538–543, Mar. 2019.



SNIGDHA SHARMA received the B.Tech. degree in electrical and electronics engineering from Gautam Buddha Technical University, Lucknow, India, in 2010, and the M.Tech. degree in power system engineering from Rajasthan Technical University, Kota, India, in 2014. She is currently pursuing the Ph.D. degree with specialization in renewable energy engineering with Galgotias University, Greater Noida, India. She worked as an Assistant Professor with the Department of Electrical and Electronics Engineering, SRM Institute of Science and Technology, Ghaziabad. She also works as an Assistant Professor with the ITS Engineering College, Greater Noida. She has published many research papers in reputed international journals and conference proceedings. Her research interests include renewable energy, solar panels, electrical machines, and power systems.



LOKESH VARSHNEY received the B.E. degree in electrical engineering from the Shri G. S. Institute of Technology and Science, Indore, India, the M.Tech. degree with specialization in electrical machines and drives from the Indian Institute of Technology (Banaras Hindu University), Varanasi, India, in 2009, and the Ph.D. degree with specialization in electrical machines and drives from the Department of Electrical Engineering, Indian Institute of Technology (BHU), in 2014. He is currently working as an Associate Professor with the School of Electrical Electronics and Communication Engineering, Galgotias University. He has published many papers in the peer-reviewed international journals and reputed conference proceedings. His research interests include electrical machines and drives, self-excited induction generator, piezoelectric transducer, solar photovoltaic, reliability engineering, and new renewable energy systems.



RAJVIKRAM MADURAI ELAVARASAN received the B.E. degree in electrical and electronics engineering from Anna University, Chennai, India, and the M.E. degree in power system engineering from the Thiagarajar College of Engineering, Madurai. He worked as an Associate Technical Operations with the IBM Global Technology Services Division. He worked as an Assistant Professor with the Department of Electrical and Electronics Engineering, Sri Venkateswara College of Engineering, Chennai. He currently works as a Design Engineer with the Electrical and Automotive Parts Manufacturing Unit, AA Industries, Chennai. He also works as a Visiting Scholar with the Clean and Resilient Energy Systems (CARES) Laboratory, Texas A&M University, Galveston, TX, USA. He has published papers in international journals, and international and national conferences. His research interests include solar PV cooling techniques, renewable energy and smart grids, wind energy research, power system operation and control, artificial intelligence, control techniques, and demand-side management. He received the Gold Medal for his master's degree. He is a recognized Reviewer in reputed journals, namely the IEEE SYSTEMS, IEEE ACCESS, the IEEE *Communications Magazine*, *International Transactions on Electrical Energy Systems* (Wiley), *Energy Sources, Part A: Recovery, Utilization and Environmental Effects* (Taylor and Francis), *Scientific Reports* (Springer Nature), *Chemical Engineering Journal* (Elsevier), and *CFD Letters and Biotech* (Springer).



AKANKSHA SINGH S. VARDHAN received the B.Tech. degree in electrical engineering from the Sam Higginbottom University of Agriculture, Technology and Sciences, Allahabad, India, in 2019. She is currently pursuing the M.E. degree in electrical engineering with specialization in power electronics with the Shri G. S. Institute of Technology and Science, Indore, India, affiliated with the Rajiv Gandhi University of Technology, Bhopal, India. Her innovative research work entitled Movable Solar Power Generator has been nominated for prestigious GYTI Award - 2020 at Rashtrapati Bhavan, New Delhi, India. She has published many research papers in reputed international journals and conference proceedings. Her research interests include power electronics and drives, renewable energy technology, SEIG and DFIG controller design, synchronous generator modeling, reliability engineering, and green energy conversion systems.



AANCHAL SINGH S. VARDHAN received the B.Tech. degree in electrical engineering from the Sam Higginbottom University of Agriculture, Technology and Sciences, Allahabad, India, in 2019. She is currently pursuing the M.E. degree in electrical engineering with specialization in power electronics with the Shri G. S. Institute of Technology and Science, Indore, India, affiliated with the Rajiv Gandhi University of Technology, Bhopal, India. Her innovative research work entitled Movable Solar Power Generator has been nominated for prestigious GYTI Award - 2020 at Rashtrapati Bhavan, New Delhi, India. She has published many research papers in reputed international journals and conference proceedings. Her research interests include renewable energy, wind energy conversion systems, DFIG controller design, design of synchronous generator, and modern aspects of power electronics.



R. K. SAKET (Senior Member, IEEE) was a Faculty Member with the Birla Institute of Technology and Science, Pilani, India, the University Institute of Technology, the Rajiv Gandhi University of Technology, Bhopal, India, and the Sam Higginbottom University of Agriculture, Technology and Sciences, Allahabad, India. He is currently a Professor with the Department of Electrical Engineering, Indian Institute of Technology (Banaras Hindu University), Varanasi, India. He has more than twenty years of academic and research experience. He is the author/coauthor of approximately 125 scientific articles, book chapters and research papers in indexed international journals and prestigious conference proceedings. He has supervised 12 Ph.D. research scholars and 45 M.Tech. students. He has delivered many technical talks and honored as a resource person of the power system reliability engineering. His research interests include reliability engineering, electrical machines and drives, power system reliability, reliability enhancement of industrial components and systems, and reliability aspects in renewable energy systems. He is a Fellow of the Institution of Engineers, India, a member of IET, U.K., and a Life Member of the Indian Society for Technical Education, New Delhi, India. He is an Editorial Board Member of the *IET Renewable Power Generation*, U.K., IEEE ACCESS, USA, the *Journal of Electrical Systems*, France, and *Engineering, Technology and Applied Science Research*, Greece. He has received many awards, honors, and recognitions for his academic and research contributions including the prestigious Gandhian Young Technological Innovation Award-2018 appreciated by the Hon'ble President of India at New Delhi, India, the Design Impact Award-2018 by Padma Vibhushan Ratan Tata at Mumbai, India, and Nehru Encouragement Award- 1988 & 1990 by the Hon'ble Chief Minister of Madhya Pradesh State Government, Bhopal.



UMASHANKAR SUBRAMANIAM (Senior Member, IEEE) was an Associate Professor, the Head of VIT, Vellore, a Senior Research and Development, and a Senior Application Engineer in the field of power electronics, renewable energy, and electrical drives. He has more than 16 years of teaching, research, and industrial research and development experience. He is currently with the Renewable Energy Laboratory, Department of Communications and Networks, College of

Engineering, Prince Sultan University, Saudi Arabia. He has published more than 250 research papers in national and international journals and conferences. He has also authored/coauthored/contributed 20 books/chapters and 15 technical articles on power electronics applications in renewable energy and allied areas. Under his guidance, 24 master's students and more than 25 bachelor's students completed the senior design project work. Also, six Ph.D. scholars completed a Ph.D. thesis as a Research Associate. He is also involved in collaborative research projects with various international and national level organizations and research institutions. His research interests include power electronics, sustainability, energy, and smart grid. He is a member of PES, PSES, and YP. He was an Executive Member, from 2014 to 2016, and the Vice-Chair of the IEEE MAS Young Professional, from 2017 to 2019. He received the Danfoss Innovator Award-Mentor, from 2014 to 2015, and from 2017 to 2018, as well as the Research Award from VIT University, from 2013 to 2018. He held positions as the Vice-Chair of the IEEE Madras Section and the Chair of the IEEE Student Activities, from 2018 to 2019. He has also received the INAE Summer Research Fellowship, in 2014. He is an Editor of *Heliyon*, *Springer Nature*, and *IEEE ACCESS*.



EKLAS HOSSAIN (Senior Member, IEEE) received the B.S. degree in electrical and electronic engineering from the Khulna University of Engineering and Technology, Bangladesh, in 2006, the M.S. degree in mechatronics and robotics engineering from the International Islamic University of Malaysia, Malaysia, in 2010, and the Ph.D. degree from the College of Engineering and Applied Science, University of Wisconsin Milwaukee (UWM). He has been involved with

several research projects on renewable energy and grid tied microgrid system with the Department of Electrical Engineering and Renewable Energy, Oregon Tech, as an Assistant Professor, since 2015. He is currently working as an Associate Researcher with the Oregon Renewable Energy Center (OREC). He is also a registered Professional Engineer (PE) of Oregon, USA. He is also the Certified Energy Manager (CEM) and a Renewable Energy Professional (REP). He has also been working in the area of distributed power systems and renewable energy integration, for last ten years. He, with his dedicated research team, is looking forward to explore methods to make the electric power systems more sustainable, cost-effective, and secure through extensive research and analysis on energy storage, microgrid systems, and renewable energy sources. He has published a number of research articles and posters in this field. His research interests include modeling, analysis, design, and control of power electronic devices, energy storage systems, renewable energy sources, integration of distributed generation systems, microgrid and smart grid applications, robotics, and advanced control systems. He is a Senior Member of the Association of Energy Engineers (AEE). He is also the winner of the Rising Faculty Scholar Award, in 2019, from the Oregon Institute of Technology for his outstanding contribution in teaching. He is also serving as an Associate Editor for *IEEE ACCESS*.

• • •